

Supporting Information

Enhanced single-ion magnet and ferroelectric properties of mononuclear Dy(III) enantiomeric pairs through the coordination role of chiral ligands

Xi-Li Li,^{*a} Ming Hu,^a Zhigang Yin,^a Cancan Zhu,^a Cai-Ming Liu,^{*b} Hong-Ping Xiao,^c and Shaoming Fang^{*a}

Experimental Section

Materials and Methods. All materials for syntheses were obtained commercially and used as received without any further purification. All the solvents used were of analytical grade. Elementary analyses for C, H and N were performed on a Perkin-Elmer 240C analyzer. IR spectra were recorded on a TENSOR27 Bruker spectrophotometer from KBr pellets in the region of 4000–400 cm⁻¹. Solid-state CD spectra were performed on a JASCO J-810 spectropolarimeter at room temperature. Crystalline samples were ground to fine powders with potassium chloride and compressed into transparent disks. The concentration of the disks was 1.00 mg per 100 mg (sample/KCl) for CD spectra measurements. The *P*–*E* hysteresis loop and leakage current of **R-1** were obtained with a Precision Multiferroic Ferroelectric Tester made by Radiant Technologies Inc. at room temperature. A single crystal of **R-1** with an approximate size of 1.5×1.0×0.8 mm³ was carefully connected to the instrument with electrodes made of Cu wire of 120 μm diameter covered by Ag conducting glue on two opposite surfaces of the crystal. Variable-temperature (2.0–300 K) direct current (dc) magnetic susceptibility measurements under an applied field of 1 kOe were accomplished on polycrystalline samples (20.46 mg for **R-1** and 17.68 mg for **R-2**) with a Quantum Design MPMS-XL5 SQUID magnetometer. Variable-temperature (2.0–15 K for **R-1** and 2.0–30 K for **R-2**) alternating current (ac) magnetic susceptibility measurements under 0 Oe/2000 Oe applied static field were performed using an oscillating field of 2.5 Oe in the different ranges of frequency.

Diamagnetic corrections were estimated from Pascal's constants for all constituent atoms.

Synthesis and Characterization. Dy(hfac)₃·2H₂O was prepared according to the literature method.¹

Synthesis of **R-1**. A solution of Dy(hfac)₃·2H₂O (82 mg, 0.1 mmol) in 15 mL n-heptane was heated to reflux for 1 h. Then the solution was cooled to 60 °C, and a dry CH₂Cl₂ (5 mL) solution of (-)-4,5-pinene bipyridine (L_R, 25 mg, 0.1 mmol) was added. The resulting mixture was stirred for 30 min and then cooled to room temperature. The mixture was filtrated and the filtrate was kept undisturbed at room temperature. After some days of slow evaporation, block-shaped and pale yellow single crystals of **R-1** were obtained. Yield: 56% based on Dy. Elemental analysis (%) calcd for **R-1** (C₃₂H₂₁F₁₈N₂O₆Dy, MW = 1034.01): C, 37.17; H, 2.05; N, 2.71. Found: C, 37.09; H, 2.11; N, 2.65. IR (cm⁻¹): 3143(w), 2947(w), 1648(s), 1503(m), 1249(s), 1223(s), 1154(s), 806(m), 653(m), 587(m).

Synthesis of **S-1**. **S-1** was obtained as pale yellow crystals by a method similar to that of **R-1**, except that (+)-4,5-pinene bipyridine (L_S) was employed instead of (-)-4,5-pinene bipyridine (L_R). Yield: 49% based on Dy. Elemental analysis (%) calcd for **R-1** (C₃₂H₂₁F₁₈N₂O₆Dy, MW = 1034.01): C, 37.17; H, 2.05; N, 2.71. Found: C, 36.96; H, 2.15; N, 2.63. IR (cm⁻¹): 3140(w), 2948(w), 1647(s), 1505(m), 1248(s), 1222(s), 1155(s), 805(m), 655 (m), 586(m).

Synthesis of **R-2**. The preparation of **R-2** follows the same procedure as for **R-1**, except that the final filtrate was stored in a refrigerator at 3 °C for two weeks to give rod-shaped pink crystals of **R-2**. Yield: 62% based on Dy. Elemental analysis (%) calcd for **R-2** (C₃₇H₂₃F₂₄N₂O₈Dy, MW = 1242.07): C, 35.78; H, 1.87; N, 2.26. Found: C, 35.69; H, 1.82; N, 2.32. IR (cm⁻¹): 3160(w), 2973(w), 1656(s), 1495(m), 1248(s), 1230(s), 1146(s), 789(m), 670(m), 593(m).

Synthesis of **S-2**. **S-2** was obtained as pink crystals by a method similar to that of **R-2**, except that (+)-4,5-pinene bipyridine (L_S) was employed instead of (-)-4,5-pinene bipyridine (L_R). Yield: 65% based on Dy. Elemental analysis (%) calcd for **S-2** (C₃₇H₂₃F₂₄N₂O₈Dy, MW = 1242.07): C, 35.78; H, 1.87; N, 2.26. Found: C, 35.70; H,

1.79; N, 2.35. IR (cm⁻¹): 3162(w), 2971(w), 1652(s), 1497(m), 1246(s), 1231(s), 1147(s), 788(m), 671(m), 591(m).

X-ray Crystallography

Single-crystal X-ray diffraction data of **R-1**, **S-1**, **R-2** and **S-2** were collected on a Bruker Smart APEX II CCD diffractometer equipped with graphite monochromatized Mo-K α radiation ($\lambda = 0.71073 \text{ \AA}$) at 153 or 173 K. The data were integrated using the *APEX2* program,² with the intensities corrected for Lorentz factor, polarization, air absorption, and absorption due to variation in the path length through the detector faceplate. Multi-scan absorption correction was applied.³ The structures were solved by direct method using SHELXS program and refined on F^2 by full-matrix least squares using SHELXL-14/7.⁴ For **R-1** and **S-1**, All non-hydrogen atoms were determined from the difference Fourier maps and refined anisotropically. Hydrogen atoms were introduced in calculated positions and refined isotropically using a riding model. For **R-2** and **S-2**, anisotropic refinement was used for all ordered non-hydrogen atoms. All hydrogen atoms were placed in calculated positions using a riding model and refined isotropically. The disorder in each $-\text{CF}_3$ groups was modelled using sets of isotropic atoms of 50% occupancy. Geometrical restraints (SADI and SIMU) were applied as necessary. The crystallographic data and refinement details for **R-1/S-1** and **R-2/S-2** are listed in Table S1. CCDC-1527501 (**R-1**), CCDC-1527502 (**S-1**), CCDC-1527499 (**S-2**) and CCDC-1527500 (**R-2**) contain the supplementary crystallographic data for this paper. These data can be obtained free of charge from The Cambridge Crystallographic Data Centre via www.ccdc.cam.ac.uk/data_request/cif.

References

1. K. Bernot, L. Bogani, A. Caneschi, D. Gatteschi and R. Sessoli, *J. Am. Chem. Soc.*, 2006, **128**, 7947.
2. Bruker (2004). *APEX2* and *SAINT*. Bruker AXS Inc., Madison, Wisconsin, USA.

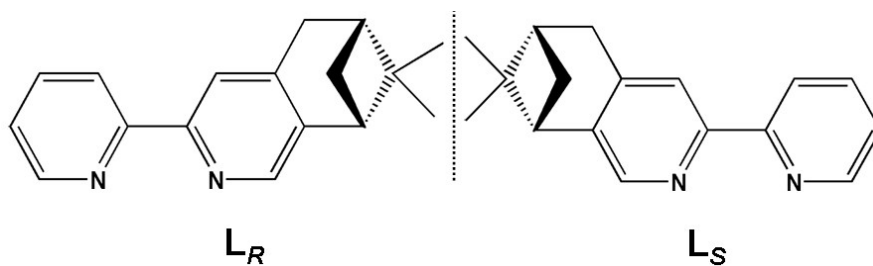
3. Bruker (2000). *SADABS*. Bruker AXS Inc., Madison, Wisconsin, USA.

4. G. Sheldrick, *Acta Cryst., Sect. C: Struct. Chem.*, 2015, **71**, 3-8.

Table S1. Crystallographic data and structure refinement parameters for **R-1**, **S-1**, **R-2** and **S-2**

	R-1	S-1	R-2	S-2
Chemical formula	C ₃₂ H ₂₁ F ₁₈ N ₂ O ₆ Dy	C ₃₂ H ₂₁ F ₁₈ N ₂ O ₆ Dy	C ₃₇ H ₂₃ F ₂₄ N ₂ O ₈ Dy	C ₃₇ H ₂₃ F ₂₄ N ₂ O ₈ Dy
Formula weight	1034.01	1034.01	1242.07	1242.07
Crystal system	Triclinic	Triclinic	Orthorhombic	Orthorhombic
Space group	<i>P</i> 1	<i>P</i> 1	<i>P</i> 2 ₁ 2 ₁ 2	<i>P</i> 2 ₁ 2 ₁ 2
<i>a</i> (Å)	12.3044(6)	12.2833(5)	18.3282(9)	18.3227(7)
<i>b</i> (Å)	13.4038(5)	13.3940(8)	21.8066(9)	21.8362(9)
<i>c</i> (Å)	13.5784(8)	13.5543(9)	11.4128(5)	11.4317(5)
α (°)	79.486(4)	79.609(5)	90	90
β (°)	65.170(5)	65.170(5)	90	90
γ (°)	88.284(4)	88.439(4)	90	90
<i>V</i> (Å ³)	1995.55(17)	1987.71(2)	4561.4(4)	4573.8(3)
<i>Z</i>	2	2	4	4
<i>D</i> _c (g/cm ⁻³)	1.721	1.728	1.809	1.804
μ /mm ⁻¹	1.999	2.007	1.787	1.782
GOF	1.020	1.066	1.044	1.053
<i>R</i> ₁ ^a / <i>wR</i> ₂ ^b	0.0509/0.1003	0.0417/0.0851	0.0375/0.0580	0.0358/0.0647
Flack parameter	0.013(10)	0.027(9)	0.028(14)	0.020(16)

$$^a R_1 = \sum ||F_o| - |F_c|| / \sum |F_o|. \quad ^b wR_2 = [\sum w(F_o^2 - F_c^2)^2 / \sum w(F_o^2)^2]^{1/2}$$



Scheme S1. Enantiomerically pure ligands (L_R and L_S).

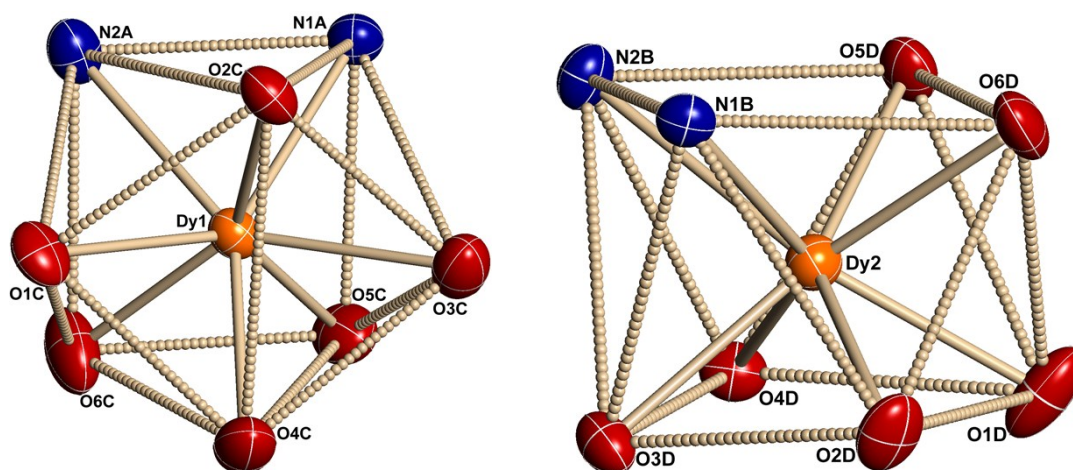


Fig. S1. Coordination geometries of two Dy(III) ions in $R-1$.

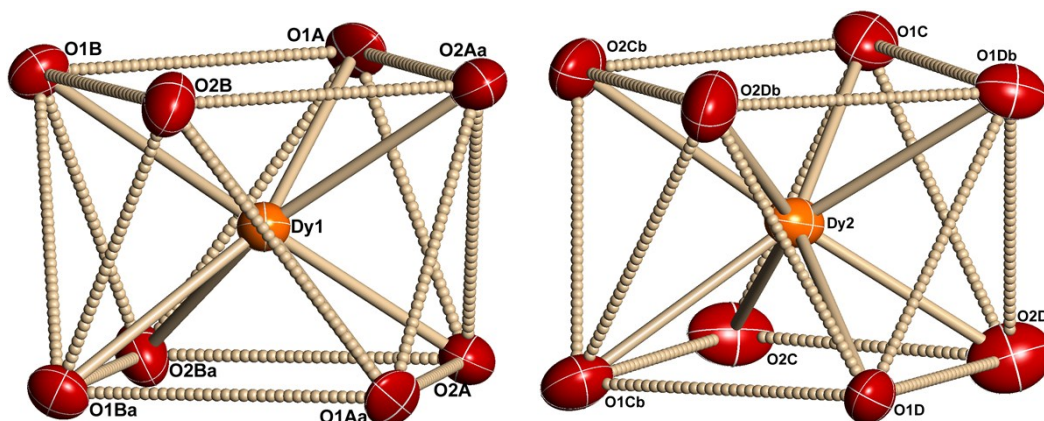


Fig. S2. Coordination geometries of two Dy(III) ions in $R-2$ (symmetry codes: $a = -x+2, -y, z$; $b = -x+1, -y, z$).

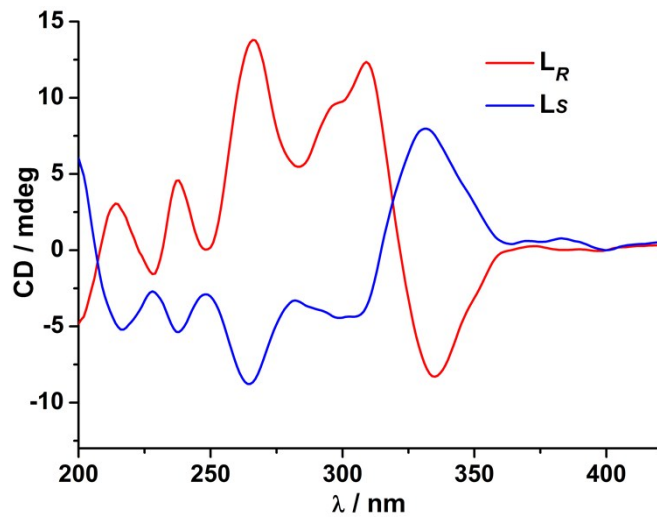


Fig. S3. Solid-state CD spectra of the free ligands L_R and L_S in KCl matrix including 1% (wt.) enantiopure crystal grains at room temperature.

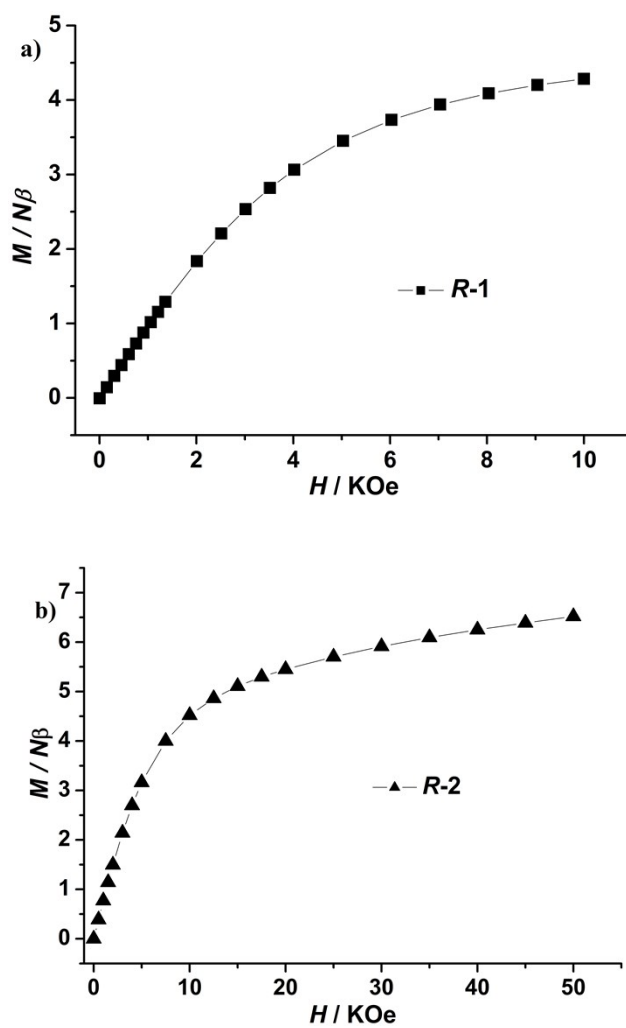


Fig. S4. Field dependence of magnetization for $R-1$ (a) and $R-2$ (b).

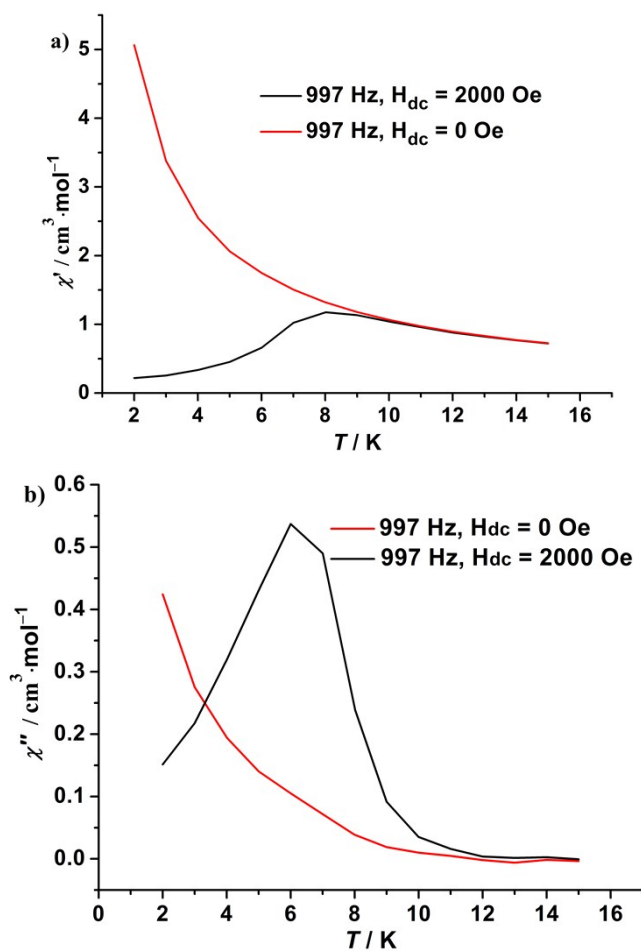


Fig. S5. Temperature dependence of the in-phase (χ') (a) and out-of-phase (χ'') (b) ac susceptibilities at 997 Hz under 0 (red line) and 2 kOe (black line) dc field for **R-1**.

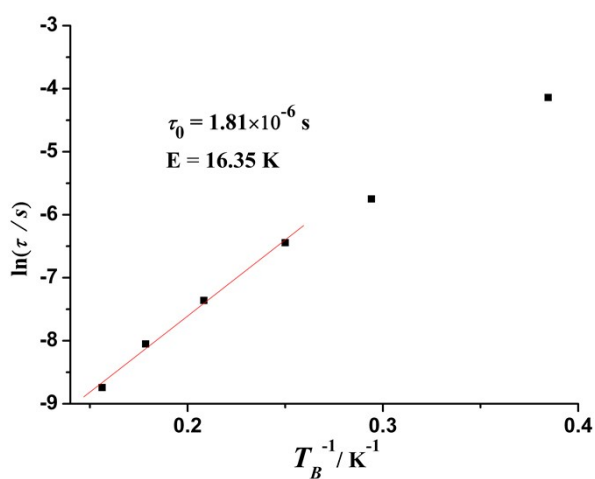


Fig. S6. Plots of $\ln(\tau)$ versus $1/T_B$ for **R-1**, the solid lines represent the fitting with the Arrhenius law.

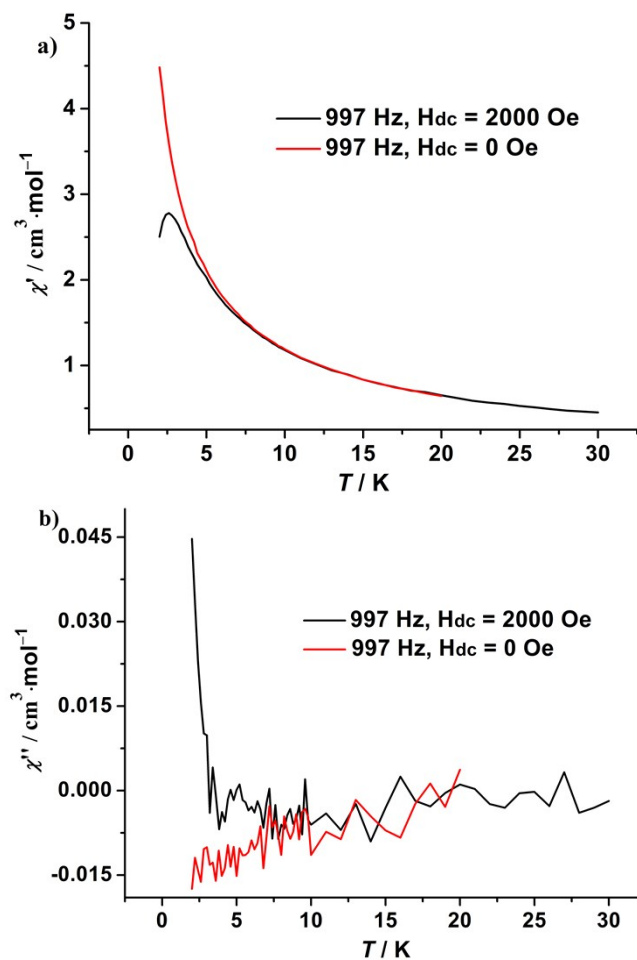


Fig. S7. Temperature dependence of the in-phase (χ') (a) and out-of-phase (χ'') (b) ac susceptibilities at 997 Hz under 0 (red line) and 2 kOe (black line) dc-field for *R-2*.

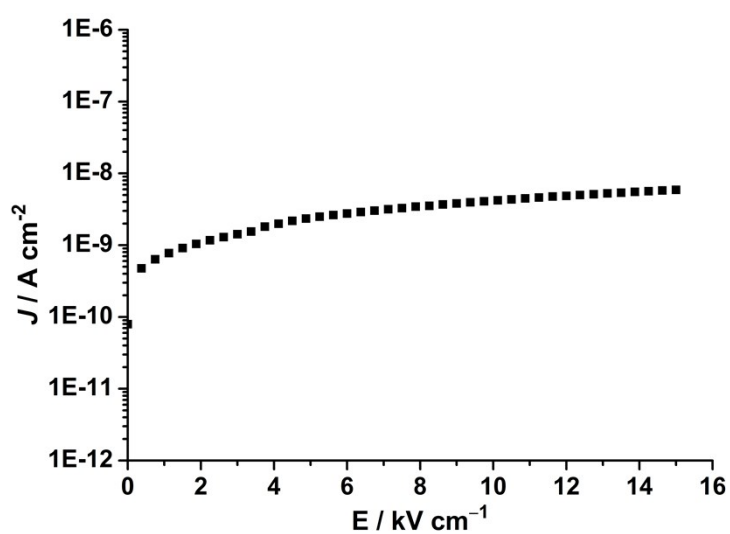


Fig. S8. Plot of the leakage currents versus the applied electric field for *R-1*.